Supernova Remnants and Supernova Feedback

Bon-Chul Koo[1], Chang-Goo Kim[2,3], Sangwook Park[4]

[1]Department of Physics and Astronomy, Seoul National University, Korea, [2]Department of Astrophysical Sciences, Princeton University, USA, [3]Center for Computational Astrophysics, Flatiron Institute, USA, [4]Department of Physics, University of Texas at Arlington, Arlington, USA

Summary

Supernova (SN) is a major feedback mechanism driving large-scale turbulence in the interstellar medium (ISM), which regulates star formation in galaxies. In recent years, it has become possible to directly simulate SN feedback in realistic multiphase ISM in full three dimensions with high resolution. Although there is an emerging consensus from these theoretical works on the evolution of supernova remnants (SNRs) and the momentum/energy input from a SN event to the ISM, observational constraints are still lacking and necessary to validate the theoretical understanding. In this presentation, we review the observations of SNRs in radiative phase in the Milky Way. There are eight SNRs where we can observe fast-expanding radiative shells in HI 21 cm line. The shell momentum is in the range of (0.5—4.5)×10^5 Msun km/s. Some of the SNRs are core-collapse SNRs interacting with molecular clouds, and they provide a template for the coupling of SN explosion energy and momentum to the inhomogeneous ISM. In two SNRs (W44 and IC 443), expanding molecular shells with momentum comparable to that of the atomic SNR shells have been also observed. We compare the observed momentum and kinetic/thermal energy of these eight SNRs with the results from 1D/3D numerical simulations in varied environments. For most SNRs, the observed momentum and kinetic energy appear to be consistent with SN explosion energy of ~10^{51} erg, while the thermal energies of several SNRs are significantly off from the theoretical evolution tracks.

Observed Parameters of HI Shells in Eight Radiative SNRs

Table 1. Parameters of Radiative HI Shells Associated with SNRs

G-name	Name	d (kpc)	v_0 (km s^{-1})	R_{sh} (pc)	v_{sh} (km s^{-1})	t_{sh} (10^4 yr)	M_{sh}(HI) (10^3 $M_\odot$)	p_{sh} (10^5 $M_\odot$ km s^{-1})	$E_{K,sh}$ (10^{50} erg)	Ref.
G34.7−0.4	W44	2.8	47	12.5	135	2.7	0.39	0.74	1.0	1
G49.2−0.7	W51C	6	62	6	96	1.8	≥ 1.2	≥ 1.6	≥ 1.5	2
G54.4−0.3[a]	···	3.3	38	19.2	59	9.5	0.58	0.49	0.28	1
		6.6	38	38.4	59	19	2.3	1.9	1.1	1
G69.0+2.7	CTB80	2	13	19	72	7.7	1.1	1.1	0.76	1
G89.0+4.7	HB 21	1.7	−12	27	61	13	2.2	1.9	1.2	this work
G189.1+3.0	IC 443	1.5	−5	7.1	100	2.1	0.49	0.69	0.69	3
G172.8+1.5	···	1.8	−20	61	55	33	5.9	4.5	2.5	4
G190.2+1.1	···	8	20	88	77	34	4.2	4.5	3.5	5

[a] The kinematic distance could be either 3.3 or 6.6 kpc using the flat rotation curve with $R_\odot = 8.5$ kpc and $\Theta_\odot = 220$ km s^{-1} (see Park et al. 2013). Junkes et al. (1992a) adopted the near distance (3.3 kpc) based on that there are star forming regions in this area at about the same distance. On the other hand, Ranasinghe & Leahy (2017) showed that there are HI 'absorption' features in the background-subtracted spectra towards the SNR radio continuum peak positions and concluded that the SNR is at the far distance (6.6 kpc). The HI brightness, however, is not spatially correlated with the SNR radio continuum (e.g., see Fig. 10 of Ranasinghe & Leahy 2017), so that the distance ambiguity is not clearly resolved. We list the parameters corresponding to both the near and far distances.

NOTE— d, v_0 = distance and systemic velocity of SNR; R_{sh}, v_{sh} = radius and expansion velocity of HI shell; $t_{sh}(\equiv 0.3R_{sh}/v_{sh})$ = characteristic age of HI shell; M_{sh}(HI)= HI mass of shell; p_{sh}, $E_{K,sh}$ = momentum and kinetic energy of HI shell including the contribution from He assuming cosmic abundance. Formal errors are $\leq 30\%$ for p_{sh} and $E_{K,sh}$. Distances are the same as those used in the references except for G54.4−0.3 and HB 21. For G54.4−0.3, see the note (b) above. For HB 21, we adopt 1.7 kpc from Byun et al. (2006).

References— (1) Park et al. (2013); (2) Koo & Moon (1997a); (3) Lee et al. (2008); (4) Koo et al. (2006); (5) Kang et al. (2014)

W44 and IC 443: Two prototypical SNRs with shocked HI and H_2

	Momentum	Kinetic energy
W44	2.14×10^5 $M_\odot$ km/s (HI: 0.74. H_2: 1.4)	1.17×10^{50} erg (HI: 1.0, H_2: 0.17)
IC 443	1.19×10^5 $M_\odot$ km/s (HI: 0.69. H_2: 0.5)	0.79×10^{50} erg (HI: 0.69, H_2: 0.1)

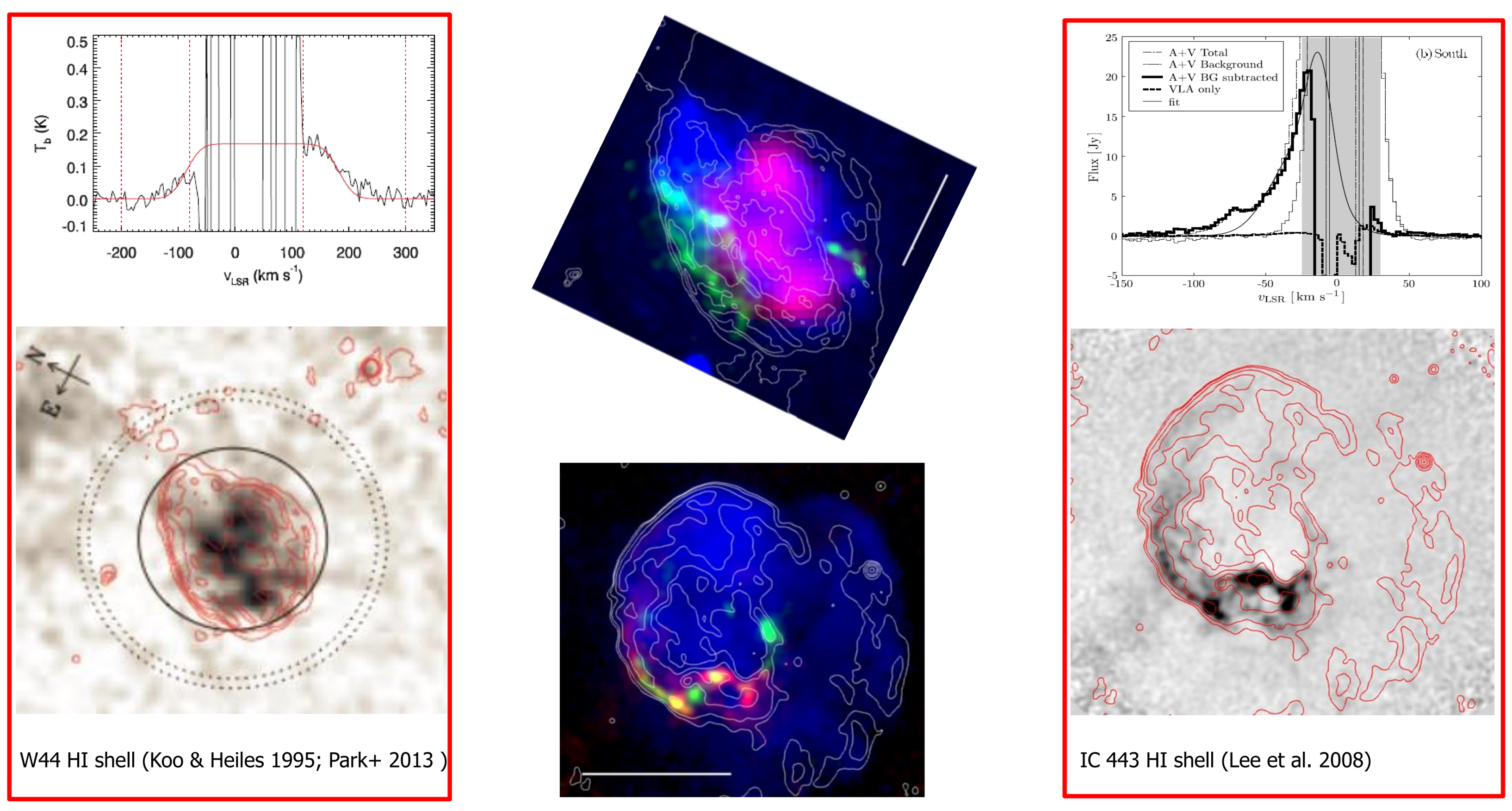

Figure 1. W44 (top) and IC 443 (bottom). Red=shocked atomic gas in Hi 21 cm emission (W44: Park et al. 2013, IC443: Lee et al. 2008), Green=shocked molecular gas in HCO+ J=1-0 line (W44: Sashida et al. 2013, IC443: Lee et al. 2012), Blue=shocked hot gas in X-ray (W44: Rho et al. 1994, IC 443: Asaoka & Aschenbach 1994), Contour=21 cm continuum (W44: Giacani et al. 1997, IC 443: Lee et al. 2008). The white scale bar in each image represents 10 pc.

Momentum, K.E., and Th.E. of Radiative SNRs: Observer's Plot

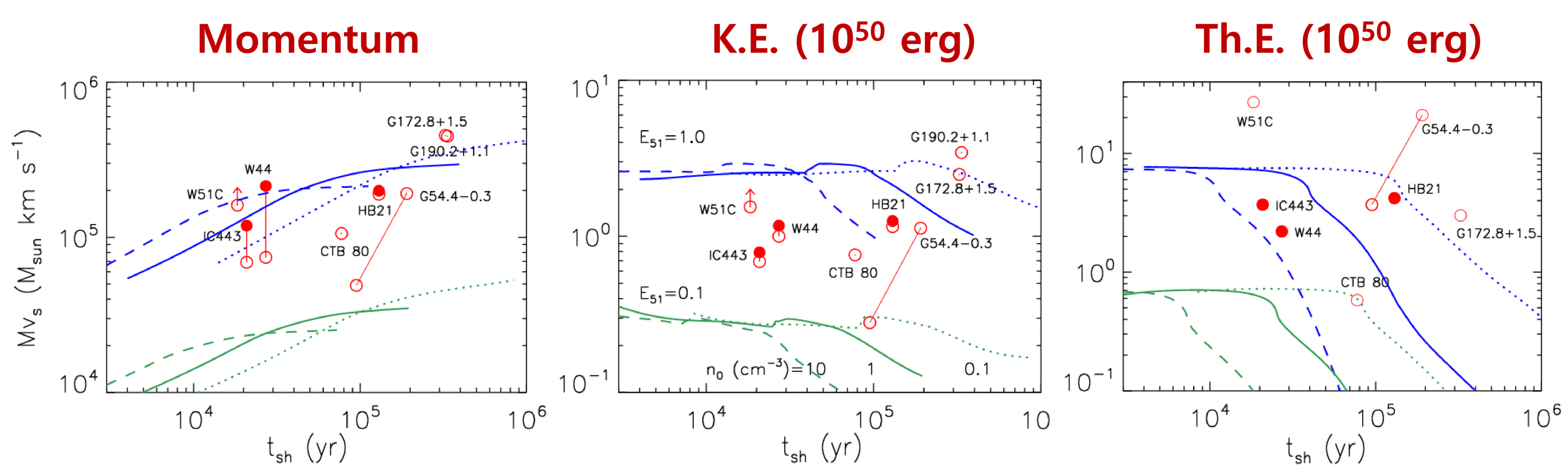

Figure 2. Observed momentum, kinetic energy, and thermal energy of SNRs with fast-expanding HI shells. The x-axis is characteristics age of HI shell t_c = $0.3R/v_s$. The empty circles represent HI component only, while the filled circles include the contribution from shocked molecular gas. Also shown are theoretical evolutionary tracks obtained from 1-D hydrodynamic simulations.

Momentum, K.E., and Th.E. of Radiative SNRs: Theoretician's Plot

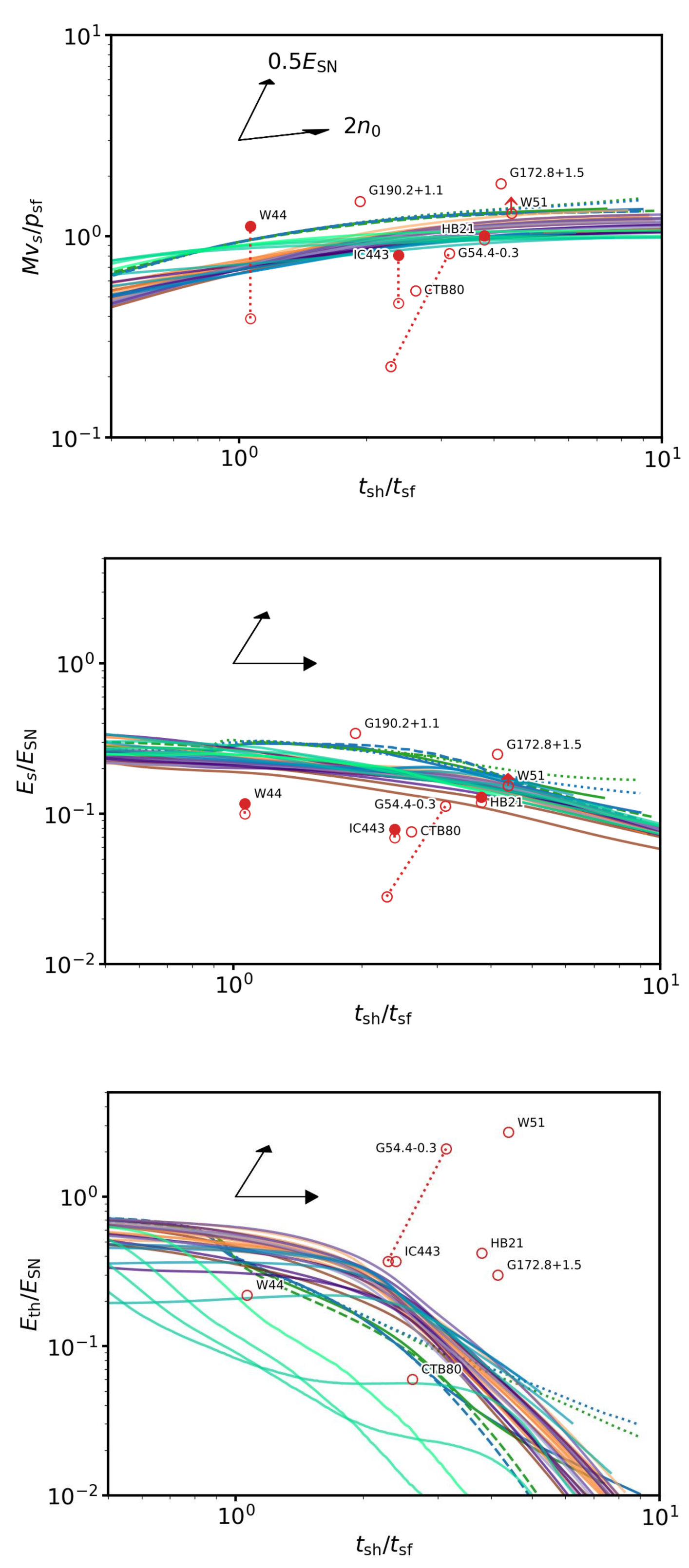

Figure 3. Observed properties normalized by the quantities at the shell formation (t_{sf} = 4.4×10^4 $E_{51}^{0.22}n_0^{-0.55}$ yr and p_{sf}=2.17×10^5 $E_{51}^{0.93}n_0^{-0.13}$ $M_\odot$ km/s; Kim & Ostriker 2015) and the explosion energy (E_{SN}=10^{51} erg). The simulated 1D evolution tracks (blue and green lines; same as Figure 2) are almost congruent for the normalized properties. The ambient medium density (n_0) is derived from observed mass (either HI only or HI+H_2) and shell size. The vectors in each panel show the directions for systematic uncertainties of E_{SN} and n_0. The evolution tracks from 3D simulations of SNRs in an inhomogeneous, two-phase medium (Kim & Ostriker 2015) with the mean number density of 1 and 10 cm^{-3} are shown as orange and purple color families (10 realizations each), respectively. The evolution tracks from 3D simulations of SNRs near the interface of two uniform media with the number density of 1 and 100 cm^{-3} (i.e., a cloud boundary; Cho et al. 2015) are shown as a teal color family (8 different explosion positions).

References: Asaoka, I., & Aschenbach, B. 1994, A&A, 284, 573; Byun, D.-Y., Koo, B.-C., Tatematsu, K., & Sunada, K. 2006, ApJ, 637, 283; Giacani, E. B., Dubner, G. M., Kassim, N. E., et al. 1997, AJ, 113, 1379; Junkes, N., Fuerst, E., & Reich, W. 1992a, A&AS, 96, 1; Kang, J.-h., Koo, B.-C., & Byun, D.-Y. 2014, JKAS, 47, 259; Kim, C.-G. & Ostriker, E. C. 2015, ApJ, 802, 99; Koo, B.-C., & Heiles, C. 1995, ApJ, 442, 679; Koo, B.-C., Kang, J.-h., & Salter, C. J. 2006, ApJL, 643, L49 ; Koo, B.-C., & Moon, D.-S. 1997a, ApJ, 475, 194; Lee, J.-J., Koo, B.-C., Yun, M. S. et al. 2008, AJ, 135, 796 ; Lee, J.-J., Koo, B.-C., Snell, R. L. et al. 2012; Park, G., Koo, B.-C., Gibson, S. J., et al. 2013, ApJ, 777, 14; Ranasinghe, S., & Leahy, D. A. 2017, ApJ, 843, 119; Rho, J., & Petre, R. 1998, ApJL, 503, L167; Sashida, T., Oka, T., Tanaka, K., et al. 2013, ApJ, 774, 10